

Transition from two-dimensional electron-hole to geminate-exciton photoluminescence in GaAs/Al_xGa_{1-x}As heterostructures under a high in-plane magnetic field

B. M. Ashkinadze and E. Cohen

Solid State Institute, Technion-Israel Institute of Technology, Haifa 32000, Israel

V. V. Rudenkov, P. C. M. Christianen, and J. C. Maan

High Field Magnet Laboratory, Institute for Molecules and Materials, Radboud University Nijmegen, Toernooiveld 7, 6525ED Nijmegen, The Netherlands

L. N. Pfeiffer

Bell Laboratories, Lucent Technologies, Murray Hill, New Jersey 07974, USA

(Received 5 March 2007; revised manuscript received 17 June 2007; published 27 August 2007)

We studied the evolution of the photoluminescence (PL) spectra in modulation-doped GaAs-based heterostructures (single quantum wells and heterojunctions) at $T_L = 1.2$ K under a high magnetic field B (up to 33 T), which was applied parallel to the two-dimensional electron gas (2DEG) layer. Under low in-plane fields, $B_{\parallel} < 7$ T, the radiative recombination of the photoexcited hole with the 2DEG gives rise to a broad PL band that shifts quadratically with B_{\parallel} . This band transforms into a narrow PL line whose peak energy E shifts linearly with B_{\parallel} in the range of 10–33 T. The slope of the linear $E(B)$ dependence was measured as $\alpha_{ex} = 0.77 \pm 0.02$ meV/T in all the studied structures. The same linear slope is also measured in the PL spectra of bulk, undoped GaAs under high B . We thus attribute the sharp PL line observed in the doped heterostructures to magnetoexcitons that are photogenerated outside the 2DEG layer by a geminate formation process. The slope of the magnetoexciton energy dependence on B_{\parallel} is compared with that measured for unbound-electron-hole Landau level transitions under a perpendicular B_{\perp} . The ratio of the measured slopes, $\alpha_{ex}/\alpha_0 \approx 0.8$, is found to be equal to the ratio of the reduced excitonic mass to the reduced cyclotron mass of GaAs.

DOI: [10.1103/PhysRevB.76.075344](https://doi.org/10.1103/PhysRevB.76.075344)

PACS number(s): 78.55.-m, 71.35.-y

I. INTRODUCTION

The radiative recombination of a two-dimensional electron gas (2DEG) with photoexcited free holes in modulation-doped heterostructures [quantum well (MDQW) and single heterojunction (SHJ)] under a perpendicularly applied magnetic field B_{\perp} gives rise to the photoluminescence (PL) (2De-h PL) spectra that contain valuable spectroscopic information on the 2DEG many-body interaction, particularly in the quantum Hall effect regime.^{1–4} The existing theoretical models for the 2De-h PL consider the recombination of the two-dimensional (2D) electron with a valence hole that is separated by a distance of d_0 from the 2DEG layer.⁵ All the dynamical processes, namely, photoexcitation, space-time evolution of the holes, as well as an exciton formation, are ignored.

The importance of dynamical processes in photoexcited heterostructures containing a 2DEG was manifested in the resonant enhancement of inelastic light scattering by the 2DEG when the photon energy is resonant with quantum-well excitons having energies higher than the Fermi energy.⁶ Dynamical processes also control the occupation of photoexcited states and give rise to the coexistence of several high-energy PL lines in the low-temperature magneto-PL spectra of MDQWs at electron filling factors $\nu < 1$.³ Another case is a remarkable transformation of the excitonic recombination spectrum in high-quality modulation-doped SHJs to 2De-h PL spectrum that occurs with increasing B_{\perp} (at $\nu < 2$).^{2,4} This was explained by the dissociation of the excitons, generated in the thick GaAs layer, at the 2DEG interface with

subsequent free hole recombination with the 2D electrons.⁴ Under low magnetic field applied *parallel* to the SHJ's interface ($B_{\parallel} \sim 1$ –2 T), 2De-h PL intensity enhancement and spectral modifications were discovered and explained by a free hole spatial redistribution.⁷

At $B=0$, an electron and a hole photogenerated at the same point of space (geminate e-h) are instantly separated since they have momenta that are equal in magnitude and opposite in direction. Then, the hole can recombine with a 2D electron or bind an electron by the bimolecular exciton formation mechanism.⁸ An applied magnetic field strongly affects the motion of the photoexcited charge carriers and their spatial distribution at rather low B .⁹ At high B , the exciton binding energy significantly increases.^{10,11}

In the present paper, we report on the effect of a high magnetic field, applied parallel to the 2DEG plane ($B_{\parallel} < 33$ T), on the photoexcited system dynamics which, in turn, affects the PL spectrum of modulation-doped heterostructures. In all the structures studied here, a transformation is observed from a broad 2De-h PL spectrum at low $B_{\parallel} < 7$ T (reported in our previous study⁷) to a narrow PL line at high B_{\parallel} . The peak energy of this line shifts linearly with B above 10 T. The slope of the linear $E(B)$ dependence was measured as $\alpha_{ex} = 0.77 \pm 0.02$ meV/T in all the studied samples. We attribute this PL line to magnetoexcitons that are photogenerated outside the 2DEG layer by a geminate formation process.

The paper is laid out as follows. Section II details the experimental procedure followed (in Sec. III) by the experimental results. In Sec. IV, we discuss the effects of B_{\parallel} on the

2De-h PL spectra in MDQWs and SHJs. In Sec. V, geminate-exciton formation under a high magnetic field is considered. The dependence of the magnetoexciton energy on B_{\parallel} is compared with that of the lowest Landau transitions between conduction and valence subbands under B_{\perp} and is analyzed in Sec. VI.

II. EXPERIMENTAL DETAILS

Several MDQW and SHJ GaAs/AlGaAs samples were studied, all grown along the (100) direction by molecular beam epitaxy. The MDQW samples contain a single quantum well of various widths (44, 25, and 20 nm), and the SHJ samples have a thick GaAs buffer layer (width of 1 μm). The n -type δ -doped layer is separated from the interface by an undoped AlGaAs layer (widths of 50–100 nm). The 2DEG density range was $n_{2D} = (0.7\text{--}2.5) \times 10^{11} \text{ cm}^{-2}$ and the 2DEG mobility was $\mu_e = (2\text{--}5) \times 10^6 \text{ cm}^2/\text{Vs}$ at 2 K. A Ti-sapphire laser illuminated the sample, and the incident light intensity (photon energy of 1.58 eV) was kept below 10^{-2} W/cm^2 . A single optical fiber was used for photoexcitation and PL collection from the sample. The sample was mounted in a cryostat and was immersed in liquid ^3He at temperature of $T_L = 1.2 \text{ K}$. The cryostat was placed in an electromagnet producing a magnetic field that reached a maximum value of 33 T. The sample plane (the 2DEG layer) was parallel to B_{\parallel} , while the photoexciting laser beam and the outgoing PL were directed perpendicularly to the sample plane. The PL was measured with a spectrometer equipped with a cooled charge coupled device, and the spectral resolution was $\sim 0.1 \text{ meV}$.

III. EXPERIMENTAL RESULTS

Figure 1(a) shows a series of PL spectra measured at increasing B_{\parallel} for the 44-nm-wide MDQW ($n_{2D} = 1 \times 10^{11} \text{ cm}^{-2}$). The panel on the left hand side displays the PL spectra at the low- B_{\parallel} range. At $B=0$, a typical 2De-h PL spectrum of MDQWs is observed.³ The PL intensity reaches a maximum at the low-energy side (E_g), and it vanishes at $E = E_g + E_F$ (E_F is the 2DEG Fermi energy). Thus, the PL bandwidth is of 3.6 meV. As B_{\parallel} increases to 8 T, the spectrum transforms into an asymmetric PL band with its maximum intensity at the high-energy side showing a blue non-linear (diamagnetic) shift.⁷

For $B_{\parallel} > 9 \text{ T}$ [right panel of Fig. 1(a)], the PL spectrum is dominated by a narrow line (width $< 0.5 \text{ meV}$) whose peak energy dependence on B , $E(B)$, is plotted in Fig. 1(b) (open circles). It is well approximated by a linear dependence with a slope of 0.79 meV/T (dashed line). The integrated PL intensity (J) is also shown in Fig. 1(b) (crosses). It varies little ($< 25\%$) in the range of 0–33 T. A similar PL behavior was observed for all the studied MDQWs; however, the B_{\parallel} values at which the linear $E(B)$ dependence starts are higher for the narrower (25 and 20 nm wide) MDQWs.

Figure 2 shows a similar series of the PL spectra obtained with the SHJ sample having $n_{2D} = 1.5 \times 10^{11} \text{ cm}^{-2}$. The main difference between the SHJ and MDQW spectra is clearly seen in the low field range, $B_{\parallel} < 3 \text{ T}$. At $B=0$, the SHJ spec-

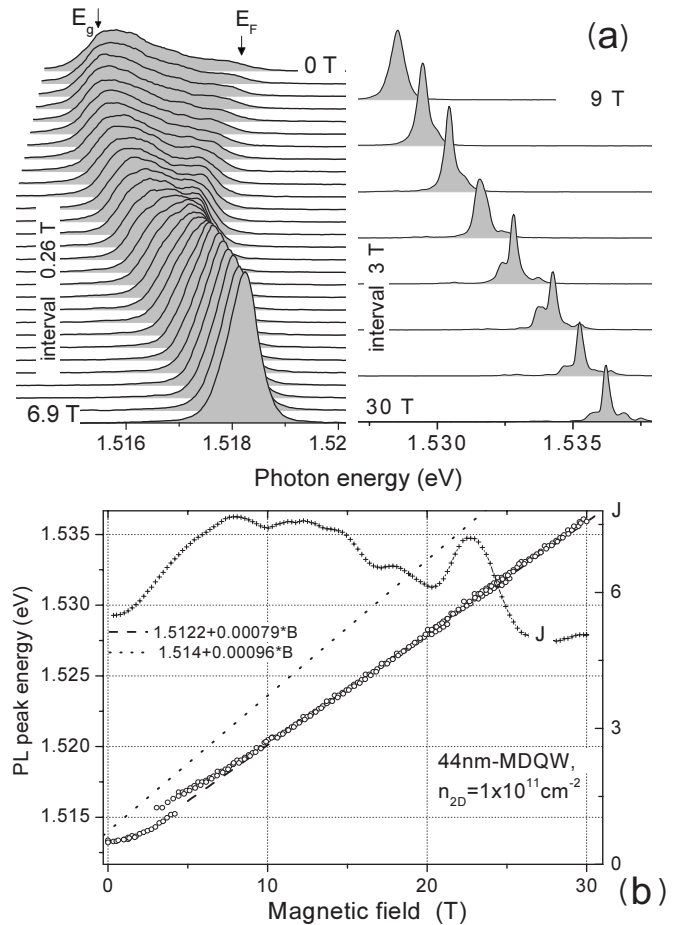


FIG. 1. (a) PL spectra of the 44-nm-wide MDQW under an in-plane magnetic field. The left panel shows the low field range spectra ($B_{\parallel} < 7 \text{ T}$), and the right panel those for higher B_{\parallel} . (b) The PL peak energy dependence on B_{\parallel} is shown by open circles, and the dashed line is the fitted straight line. The dotted line shows the B_{\perp} dependence of the energy of the lowest electron-hole Landau transition. The crosses are the integrated PL intensity J (in arbitrary units) dependence on B_{\parallel} .

trum consists of two narrow excitonic lines that originate in the 1- μm -thick GaAs buffer layer: the high-energy line is due to free excitons and the low-energy one to localized excitons. The very weak, broad band below the excitons (marked 2De-h PL) is due to the radiative recombination of the 2DEG with itinerant photoexcited holes.⁴ [The recombination channels that give rise to the various PL bands are schematically depicted in Fig. 5(a)]. The intensity of the 2De-h PL at $B=0$ is very low (in SHJs having $n_{2D} > 1 \times 10^{11} \text{ cm}^{-2}$), because the strong built-in electric field E_{hj} accelerates the holes away from the GaAs/AlGaAs interface where the 2DEG forms.¹²

A remarkable modification of the SHJ PL spectrum upon applying a low in-plane field ($B_{\parallel} < 4 \text{ T}$) is seen in left panel of Fig. 2. With increasing B_{\parallel} , the 2De-h PL intensity increases while the excitonic PL intensity diminishes. The spectrum transforms into a strongly asymmetric band with its maximum at the high-energy PL side, and the excitonic lines are hardly seen.⁷ With further field increase ($B_{\parallel} > 8 \text{ T}$, right panel of Fig. 2), the PL spectrum narrows and becomes sym-

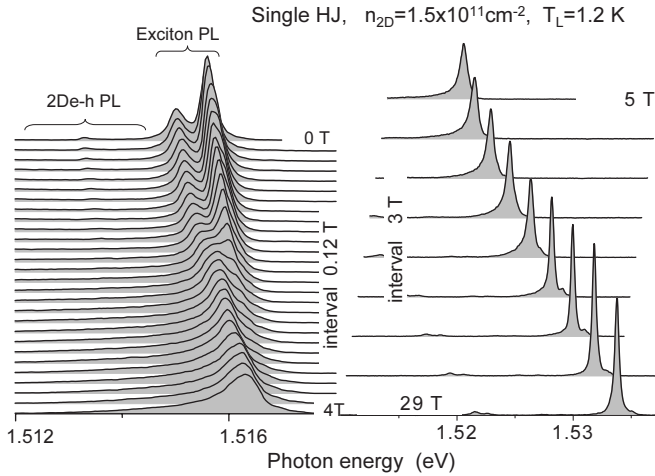


FIG. 2. PL spectra of a SHJ under in-plane B . The low-field spectra (left panel) show a transformation from the excitonic PL to 2De-h PL occurring at $B_{\parallel} < 3$ T. At higher B_{\parallel} (right panel), the 2De-h PL band transforms into a geminate-exciton PL line.

metric. The PL peak energy shows an $E(B_{\parallel})$ dependence that is similar to that of the MDQW. Similar PL evolution with B_{\parallel} was observed for several other SHJ samples that were studied here.

Since the SHJs contain a $1\text{-}\mu\text{m}$ -thick, undoped GaAs buffer layer, we found it beneficial to compare their magneto-PL spectra under B_{\parallel} with those of a bulk, undoped GaAs layer ($10\text{-}\mu\text{m}$ -thick). Figure 3 (right panel) displays some magneto-PL spectra of this GaAs layer, observed at several B values. At $B=0$, the spectrum consists of free (FE) and bound exciton PL lines,¹² and as B increases, the free exciton line dominates the spectrum. Under high fields ($B > 15$ T), it splits into two lines. The peak energy E dependence on B (of the free exciton line and of the center of gravity for the two split lines) is plotted in Fig. 3 (open

circles). This curve is fitted with a quadratic (diamagnetic) exciton shift for $B < 7$ T, and at higher fields, it is well approximated by a linear function with a slope of 0.77 meV/T (solid line).

In Fig. 4(a), we compare representative PL spectra of two SHJs having different n_{2D} , measured at $B_{\parallel}=6$ and 26 T, with those of the undoped GaAs sample. The SHJ spectra show similar shifts as those of the undoped GaAs sample, but the latter has impurity-bound exciton bands, which are lacking in the former. Also, the PL line of the SHJ with higher n_{2D} is observed at lower energy than that of the lower density SHJ, and both are still lower than the GaAs free magnetoexciton. The $E(B)$ dependence of these three samples is compared in Fig. 4(b). In the low- B range [inset of Fig. 4(b)], the $E(B)$ dependencies for the SHJs follow the diamagnetic shift of free (bound) excitons of bulk GaAs (at $B < 4$, the FE peak energies coincide for all three samples). As the excitonic PL lines in the SHJs are transformed into the 2De-h PL band, the PL peak energy in the range of 2–10 T shows a diamagnetic shift, which is weaker than that of the free exciton.

In the range of 10–33 T, the PL line positions of the studied SHJs samples move almost in parallel to that of the bulk FE line. All $E(B)$ dependencies are approximated by straight lines with a slope of $0.77 \pm 0.02\text{ meV/T}$. The energy differences between the $E(B)$ line for the SHJs and the bulk GaAs sample are $\approx 1\text{ meV}$ [for SHJ(a), low n_{2D}] and $\approx 2\text{ meV}$ [for SHJ(b), high n_{2D}] as seen in Fig. 4(b). It is important to notice that the integrated PL intensity J varies only slightly in the entire range of 0–33 T.

IV. 2De-h SPECTRAL CHANGE UNDER IN-PLANE $B_{\parallel} < 10$ T

Before discussing the PL spectra that are observed under a high in-plane magnetic field in various modulation-doped heterostructures, we briefly review the physical model of a

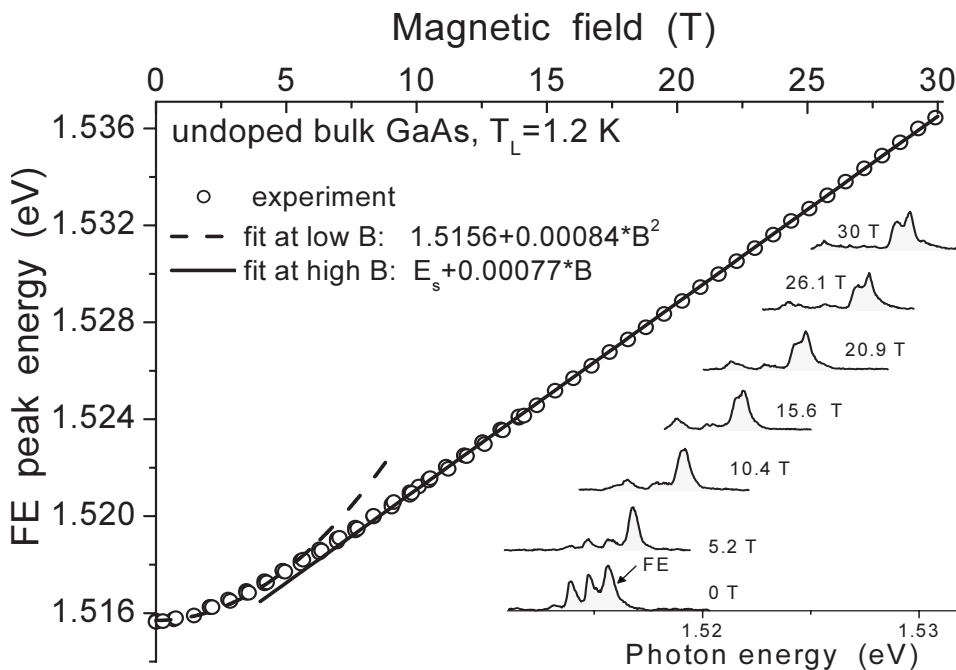


FIG. 3. PL spectra of an undoped, bulk GaAs sample (right panel). The most intense line is the free exciton, and its energy dependence on magnetic field, $E(B)$, is presented by open circles. Line fittings are shown: exciton diamagnetic shift at low B and a linear shift at high B .

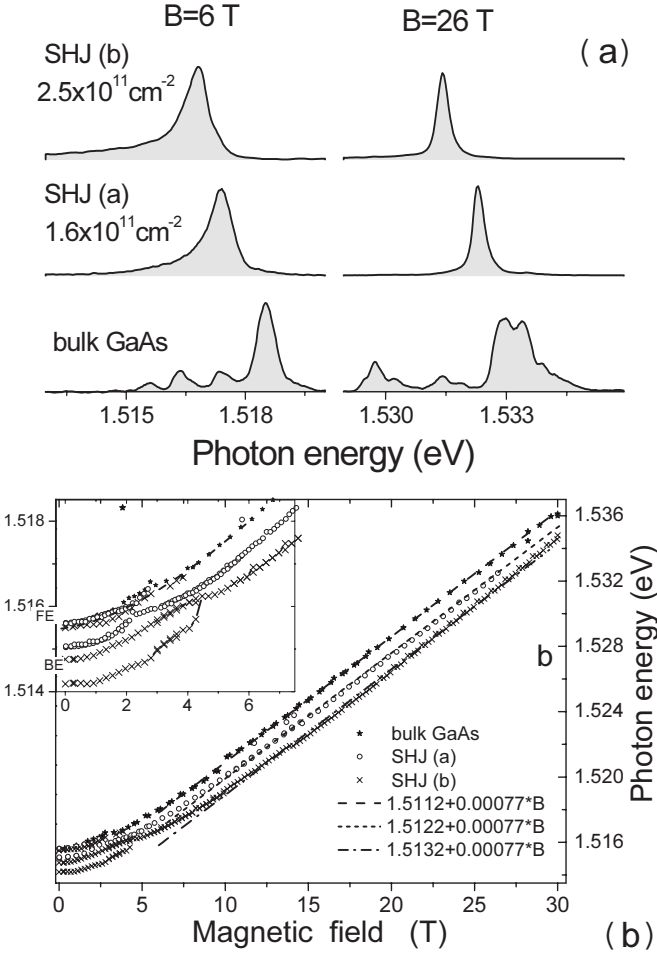


FIG. 4. (a) The PL spectra of two SHJs having different n_{2D} and an undoped, bulk GaAs sample at two B_{\parallel} values. (b) The PL peak energy dependencies on B for these samples. The inset shows the low- B_{\parallel} range.

2DEG subjected to a built-in electric field E_{hj}^z and an in-plane magnetic field B_{\parallel}^x (see Fig. 5). This crossed field configuration causes an electron drift in the y direction, and it leads to a shift of the electron subband minimum to high wave vectors k_B^y and to an increase in the in-plane electron effective mass (in the y direction).^{13–15}

We reported recently on the effect of an in-plane magnetic field on the 2De-h PL spectra of heterostructures in the range of $B_{\parallel} < 7 \text{ T}$. The 2De-h PL spectral modifications with increasing B_{\parallel} were then explained by invoking direct optical transitions in an indirect band gap structure that results from the shift in k space of the conduction and valence subbands by $k_B^y = d_0/L_B^2$ [as shown schematically in Fig. 5(b)]. Here, d_0 is the 2De-h spatial separation and L_B is the magnetic length. In addition, the 2DEG Fermi energy decreases due to the electron effective mass increase. For such an indirect band gap structure, the direct optical transitions giving rise to the same emitted photon energy involve the conduction- (and valence-) band states of various energies (according to the momentum and energy conservation laws). This is in contrast to the optical transitions occurring in the direct band gap structure (e.g., at $B=0$), and thus, a dramatic modification of the 2De-h spectrum is caused by applying in-plane B_{\parallel} .⁷

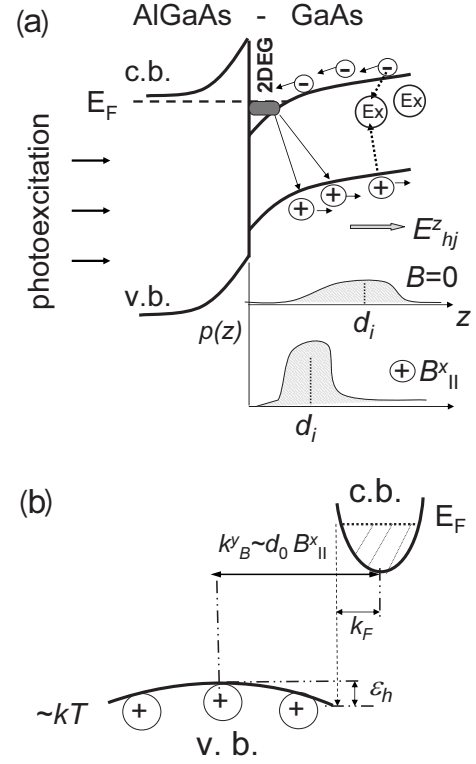


FIG. 5. (a) The physical processes in photoexcited single heterojunctions; $p(z)$ is the photohole distribution. (b) Schematic of the 2De-h recombination in the indirect band gap formed in the presence of a high in-plane B .

The PL spectra for the 44-nm-wide MDQW [Fig. 1(a), left panel] show spectral modifications similar to those previously studied for the 25-nm-wide MDQW.⁷ However, the PL transformations for the 44-nm-wide MDQW are observed at lower B_{\parallel} , and this is due to larger electron-hole separation since $k_B^y \propto d_0 \cdot B_{\parallel}$. Moreover, the 2De-h PL band in the studied sample significantly narrows from 3.6 meV ($B=0$) to 0.9 meV at 7 T. Such a narrowing at large k_B^y was also obtained in the developed model.⁷

In SHJs, the in-plane magnetic field causes spatial redistribution of the photoexcited holes, in addition to the band gap modification discussed above. Electrons and holes (e-h) are photoexcited across the whole 1- μm -wide undoped buffer GaAs layer. The photoexcited holes drift in the built-in electric field E_{hj} formed by the positive charged donors in the AlGaAs barrier. Assuming homogeneous e-h photogeneration in the GaAs layer with a rate G , a steady-state spatial distribution of free holes along the z axis, $p(z)$, in the presence of the constant E_{hj} , can be obtained from the equation

$$G - p/\tau + \mu E_{hj}(dp/dz) = 0, \quad (1)$$

and its solution is as follows:

$$p(z) = G\tau[\exp(z/L_E) - 1]. \quad (2)$$

Here, τ is the hole lifetime and $L_E = \mu\tau E_{hj}$ is the drift length (μ is the hole mobility). The expected spatial distribution of the itinerant holes is schematically drawn in Fig.

5(a). At large z , $p(z)$ decreases since E_{hj} decreases and the binding of e-h pairs into excitons becomes important. It is evident that such a hole distribution results in a low 2De-h PL intensity and an intense GaAs exciton PL as is seen in the PL spectrum shown at $B=0$ in Fig. 2.

As the in-plane B_{\parallel} increases, the distance between the itinerant photoholes and the 2De decreases. Indeed, the hole exhibits a cycloidal motion along the y axis, and the hole drift in the z direction is suppressed. This results in the hole density redistribution that is schematically shown in Fig. 5(a), and the 2De-h PL intensity increases at the expense of the bulk excitonic PL.

In contrast to the MDQWs, however, the 2De-h PL of SHJ consists of the radiative recombination of the 2De-h pairs that have various spatial separations d_i , and therefore, it is a sum of spectra corresponding to various $k_B^y = d_i/L_B^2$. Under B_{\parallel} , this gives rise to the distinct 2De-h PL spectrum that has a long low-energy tail (for example, as seen in Fig. 2 at 4 T).

At high B_{\parallel} (>8 T), the PL line of both SHJ and MDQW samples significantly narrows [Figs. 1(a), 2, and 4(a)]. The $E(B)$ dependence of this line becomes linear and can be characterized by nearly the same slopes for all the studied samples.

The nature of the narrow PL lines appearing at high B_{\parallel} must be different from the 2De-h recombination. At $B_{\parallel} > 8$ T, the conduction and valence subbands are shifted in k space by a k_B value that exceeds the Fermi wave vector k_F , and the highest kinetic energy of the hole participating in the direct optical transition [see Fig. 5(b)], $\varepsilon_h = [\hbar(k_B - k_F)]^2/2m_h$, increases with B_{\parallel} . However, the occupation of these states exponentially decreases if the photoexcited holes have a thermalized Boltzmann distribution near the top of the valence band. Thus, at $T_L = 1.2$ K, only a few photoexcited, nonthermalized holes can participate in the direct optical transitions with the 2DEG, and the radiative lifetime would greatly increase with B_{\parallel} . It would result in a strong PL quenching at high B_{\parallel} in the presence of any nonradiative recombination channels.

A similar PL quenching was observed in the spatially indirect exciton PL of double quantum-well structures under an in-plane B .¹⁶ However, no reduction in the integrated PL intensity with B_{\parallel} up to 22 T was recently detected in similar double QW structures.¹⁷ This fact was explained by a better sample quality and introducing a localized exciton recombination mechanism that relaxes the wave vector conservation for the indirect exciton radiative recombination.

In the studied MDQWs and SHJs, the integrated PL intensity does not quench by the high B_{\parallel} [up to 33 T, Fig. 1(b)]. We cannot attribute this to any localization since the radiative recombination of localized holes with the 2DEG would result in a broad 2De-h PL band (as was observed in Ref. 18), in contradiction with the experimental results in Figs. 1 and 2. We explain the observed spectral PL evolution in MDQWs and SHJs under high B_{\parallel} (Figs. 1–4) by a change-over of the 2De-h radiative recombination into the PL of free, geminate-formed excitons.

V. GEMINATE-EXCITON FORMATION UNDER STRONG MAGNETIC FIELD

In the previous discussion of the 2De-h PL modification induced by a magnetic field, it was assumed that an electron and a hole photogenerated at the same point of space (geminate e-h) are instantly separated, and then, the hole can recombine with the 2DEG. The geminate electron and hole moving in opposite directions lose their mutual memory (and thus become unbound) after a time interval of θ . This time can be estimated using the model of electron capture by an attractive center (hole).¹⁹ In this model, the electron is captured if it loses the energy of kT_L being in the sphere of radius $R_T = e/\kappa kT_L$ surrounding the hole (κ is the dielectric constant).

At $B=0$, the geminate e-h pair will be separated by a distance of R_T for $\theta = R_T/V \sim 10^{-11}$ s (taking a relative velocity of $V \sim 10^7$ cm/s and $T_L = 2$ K). This time is much shorter than the energy relaxation time due to electron-phonon scattering, $\tau_e \approx \tau_m(kT_L/4m_e s^2) \sim 5 \times 10^{-10}$ s.²⁰ Here, s is the sound velocity and $\tau_m \sim 4 \times 10^{-11}$ s is the momentum relaxation time for electrons having mobility above 10^6 cm²/V s. Since $\theta \ll \tau_e$, the geminate e-h pair does not directly form an exciton and is separated. Thus, the 2De-h recombination takes place before the slow-acting bimolecular exciton formation occurs.^{8,21}

Under a high magnetic field, the geminate-exciton formation process controls the PL of semiconductors. The importance of geminate recombination was considered in several theories,^{9,22} in connection with the observed enhancement of PL intensity²³ and Raman light scattering efficiency²⁴ under a magnetic field.

We propose that the observed PL spectral evolution under high magnetic fields (Figs. 1–4) is due to a transformation of the 2De-h PL into the PL of geminate-formed magnetoexcitons.

In the plane perpendicular to the magnetic field, the photogenerated electron and hole move on the same circular orbits and in the opposite directions (or on close cycloids in the case of E_{hj}^z and B_{\parallel}^*). Their separation in this plane occurs by a diffusion process with a coefficient $D = r_B^2/\tau_m$, where r_B is the cyclotron radius.²⁰ The geminate electron-hole pair conserves their mutual memory during a time of $\theta = R_T^2/D = (R_T/r_B)^2 \tau_m$. At $B > 5$ T, θ is of the order of $10^{-7} - 10^{-6}$ s, and $\theta \gg \tau_e$. Thus, the geminate electron and hole lose energy and bind into an exciton before they are separated (the geminate pair moving parallel to B , in general, will be separated). It is worth noting that the geminate-exciton formation mechanism is most important for polymers and semiconductors having low carrier mobility where geminate pairs are slowly separated even in the absence of B .²⁵

Thus, we attribute the narrow PL lines emerging in all MDQWs and SHJs under high B to free, geminate-formed magnetoexcitons. The weak integrated PL intensity dependence on B_{\parallel} measured in all the studied samples [Fig. 1(b)] is also explained by the transformation of the indirect in k -space 2De-h PL to the geminate-formed free magnetoexciton PL. This underlines the importance of the dynamical processes in controlling the PL spectrum. Geminate-formed magnetoexcitons also play an important role in the interpre-

tation of the spectral PL evolution that was extensively studied under B_{\perp} .¹⁻⁴

VI. FREE EXCITONS UNDER A HIGH MAGNETIC FIELD

In the range of $B_{\parallel}=10\text{--}33$ T, all the studied GaAs-based structures exhibit a linear $E(B_{\parallel})$ dependence with the same slope, $\alpha_{ex}=0.77\pm 0.02$ meV/T (Figs. 1–4). For the SHJ samples subjected to a perpendicularly applied field B_{\perp} , the high-energy PL line (free exciton PL) has an $E(B_{\perp})$ dependence which is similar to that of $E(B_{\parallel})$, while the low-energy, 2De-h PL line shows a different $E^{LL}(B_{\perp})$ dependence.⁴ The latter is determined by the shift of the lowest-energy electron-hole Landau transition E^{LL} with increasing B_{\perp} .

In MDQWs subjected to B_{\perp} , the main (lowest energy, 2De-h) PL line follows the $E^{LL}(B_{\perp})$ dependence at low B_{\perp} (at filling factors $\nu > 2$). At higher B_{\perp} (above ~ 10 T), excitonlike lines (charged and neutral excitons) dominate the PL spectrum of GaAs-based MDQWs (having $n_{2D} \leq 2 \times 10^{11}$ cm⁻²). Their $E(B_{\perp})$ can also be approximated by a nearly linear dependence that has the same slope of 0.77 ± 0.02 meV/T.^{3,26}

Such a universal linear $E(B)$ dependence of the geminate-formed exciton PL line observed at high B deserves special consideration. Its slope α_{ex} is likely to be an important inherent parameter which is determined by the B dependence of the exciton binding energy $\delta E_x(B)$, since $E(B)=E^{LL}(B)-\delta E_x(B)$.

For an unbound electron-hole pair, the energy of the optical transitions between the lowest Landau levels of the conduction and valence subbands varies as

$$E^{LL}(B_{\perp}) = E_{g0} + (1/2)(\hbar e/c \mu_c) B_{\perp}, \quad (3)$$

where E_{g0} is the band gap energy at $B=0$ and $\mu_c = m_e m_h / (m_e + m_h)$ is the reduced electron-hole cyclotron effective mass. In the approximation of simple, parabolic conduction and valence bands,²⁷ the slope of the linear $E^{LL}(B_{\perp})$ dependence is $\alpha_0 = (1/2)(\hbar e/c \mu_c) = 0.96$ meV/T for electron and hole cyclotron effective masses of bulk GaAs, $m_e = 0.068 m_0$ and $m_h = 0.52 m_0$.²⁸ For a 20-nm QW, $\alpha_0 = 1.02$ meV/T (for $m_h = 0.35 m_0$).²⁹

The dotted line in Fig. 1(b) shows the $E(B_{\perp})$ dependence of the lowest electron-hole Landau level transition for the 44 nm MDQW. From this line, we get $\alpha_0 = 0.96$ meV/T, and thus $\mu_c = 0.06 m_0$. This determines the hole cyclotron mass value of $\approx 0.52 m_0$.

The obtained $E(B)$ dependence for the geminate-formed exciton PL suggests that the magnetoexciton binding energy δE_x depends almost linearly on B in the range of 10–33 T. The $\delta E_x(B)$ dependence was analyzed in several theoretical approximations.¹⁰ For simple band structures, these theories do not predict a linear $E(B)$ [or $\delta E_x(B)$] dependence in the range of

$$\gamma = \alpha_0 B / \delta E_x(0) = [\hbar^3 \kappa^2 / (\mu_c^2 e^3 c)] B \sim 2 - 7, \quad (4)$$

which corresponds to the B range of 10–33 T at $\mu_c = 0.06 m_0$ and $\kappa = 13$.

Subsequent theories (see references in Ref. 11) took into account the complexity of the GaAs valence band, and the

analysis of the $E(B)$ dependence was usually performed by using the theoretically calculated B dependence of several fitting parameters of the GaAs valence band.^{11,30}

The universal $E(B)$ dependence for the exciton PL peak observed for all the studied GaAs-based structures can be presented as $E(B) = E_s + \alpha_{ex} B$, where E_s is the energy extrapolated to $B=0$, and an “excitonic” slope is introduced as follows:

$$\alpha_{ex} = \alpha_0 \mu_0 / \mu_c. \quad (5)$$

From the measured α_{ex}/α_0 ratio of ≈ 0.8 , we get $\mu_0 \approx 0.046 m_0$. Remarkably, this value coincides with the reduced excitonic mass $\mu_0^{-1} = m_e^{-1} + (m_h^s)^{-1}$ that defines the exciton Bohr radius.^{11,31} Here, m_h^s is the hole effective mass in spherical valence-band approximation. Thus, the simple empirical expression [Eq. (5)] describes well the PL exciton energy behavior under a high magnetic field.

At low B ($\gamma \ll 1$), the $E(B)$ dependence shown in Fig. 3 is described by the expression for the excitonic diamagnetic shift obtained by perturbation theory: $E(B) = E_{g0} + \Delta E_x [0.5\gamma^2 - 1]$ (see p. 202 in Ref. 11). The dependence shown by the dotted curve in Fig. 3 fits well the experimental data at $B < 7$ T with the γ value [Eq. (4)] calculated for the cyclotron μ_c value, while the exciton binding energy is $\Delta E_x = e^4 \mu_0 / 2 \hbar^2 \kappa^2 = 4.2$ meV using the μ_0 value. Thus, the magnetoexciton energy dependence in the entire B range is obtained by two simple, empirical expressions that use three well-known GaAs parameters, μ_0 , μ_c , and κ .

As seen from Fig. 4, the $E(B_{\parallel})$ dependence for the geminate-formed excitons in the SHJs shifts to lower energy with increasing the 2DEG density. This can be explained invoking a shallow well for the excitons that is formed near the interface with the 2DEG in the SHJs.³² Due to the built-in electric field gradient, the excitons photoexcited in the GaAs buffer layer drift to the higher E_{hj} region and are localized in the well. Geminate-formed excitons are likely to occupy this well, and the localization energy increases as E_{hj} becomes higher (for increased n_{2D}); thus, the exciton PL peak shifts to low energy.

VII. CONCLUSIONS

The effects of a magnetic field, applied parallel to the 2DEG layer, on the low-temperature photoluminescence spectrum of modulation-doped, GaAs-based heterostructures (single quantum wells and heterojunctions), are studied for B_{\parallel} up to 33 T. At $B_{\parallel} < 7$ T, the remarkable changes of the 2DEG free hole PL spectra are due to the B_{\parallel} -induced direct-indirect band gap transformation.^{7,13,14}

At $B_{\parallel} > 10$ T, the PL spectrum observed in all the studied modulation-doped heterostructures as well as undoped, bulk GaAs consists of a narrow PL line whose peak energy E shifts linearly with B . We attribute this sharp PL line to magnetoexcitons that are photogenerated by a geminate formation process.

The linear $E(B)$ dependence of the geminate-formed

magnetoexcitons is characterized by a universal slope of $\alpha_{ex}=0.77\pm 0.02$ meV/T. It is different from that of unbound-electron-hole Landau level transitions under a perpendicular B . The ratio of these slopes ($\alpha_{ex}/\alpha_0\approx 0.8$) is equal to the ratio of the reduced excitonic mass to the reduced cyclotron mass, μ_0/μ_c of GaAs. We show that two simple, empirical expressions based on three well-known GaAs parameters μ_0 , μ_c , and κ , allow us to describe the magnetoexciton energy dependence in the entire B range.

ACKNOWLEDGMENTS

The research at the Technion was done in the Barbara and Norman Seiden Center for Advanced Optoelectronics and was supported by the Israel-US Binational Science Foundation (BSF), Jerusalem. Part of this work is supported by the EU Enhancing Access to Research Infrastructures (ARI) Action of the Improving Human Potential (IHP) Programme, Contract No. HPRI-CT-1999-0003. B.M.A. acknowledges support by a grant from the KAMEA Program.

- ¹D. Heiman, B. B. Goldberg, A. Pinczuk, C. W. Tu, A. C. Gossard, and J. H. English, *Phys. Rev. Lett.* **61**, 605 (1988); D. Heiman, A. Pinczuk, H. Okamura, M. Dahl, B. S. Dennis, L. N. Pfeiffer, and K. W. West, *Physica B* **201**, 315 (1994).
- ²A. J. Turberfield, S. R. Haynes, P. A. Wright, R. A. Ford, R. G. Clark, J. F. Ryan, J. J. Harris, and C. T. Foxon, *Phys. Rev. Lett.* **65**, 637 (1990); I. V. Kukushkin and V. B. Timofeev, *Adv. Phys.* **45**, 147 (1996).
- ³B. M. Ashkinadze, E. Linder, E. Cohen, A. B. Dzyubenko, and L. N. Pfeiffer, *Phys. Rev. B* **69**, 115303 (2004); B. M. Ashkinadze, V. V. Rudenkov, P. C. M. Christianen, J. C. Maan, E. Linder, E. Cohen, and L. N. Pfeiffer, *Phys. Status Solidi C* **1**, 514 (2004).
- ⁴B. M. Ashkinadze, V. Voznyy, E. Cohen, A. Ron, and V. Umansky, *Phys. Rev. B* **65**, 073311 (2002); B. M. Ashkinadze, E. Linder, E. Cohen, V. V. Rudenkov, P. C. M. Christianen, J. C. Maan, and L. N. Pfeiffer, *ibid.* **72**, 075332 (2005).
- ⁵E. I. Rashba and M. E. Portnoi, *Phys. Rev. Lett.* **70**, 3315 (1993); A. H. MacDonald, E. H. Rezayi, and D. Keller, *ibid.* **68**, 1939 (1992); J. J. Palacios and H. A. Fertig, *ibid.* **79**, 471 (1997).
- ⁶G. Danan, A. Pinczuk, J. P. Valladares, L. N. Pfeiffer, K. W. West, and C. W. Tu, *Phys. Rev. B* **39**, 5512 (1989).
- ⁷B. M. Ashkinadze, E. Linder, E. Cohen, and L. N. Pfeiffer, *Phys. Rev. B* **71**, 045303 (2005).
- ⁸V. N. Abakumov, V. I. Perel, and I. N. Yassievich, *Zh. Eksp. Teor. Fiz.* **78**, 1240 (1980); [*Sov. Phys. JETP* **51**, 626 (1980)].
- ⁹I. A. Merkulov and V. I. Perel, *J. Lumin.* **60&61**, 293 (1994).
- ¹⁰Y. Yafet, R. W. Keyes, and E. N. Adams, *J. Phys. Chem. Solids* **1**, 137 (1956); L. P. Gorkov and I. E. Dzyaloshinskii, *Zh. Eksp. Teor. Fiz.* **53**, 717 (1967); [*Sov. Phys. JETP* **26**, 449 (1968)].
- ¹¹D. Bimberg, *Adv. Solid State Phys.* **17**, 195 (1977).
- ¹²B. M. Ashkinadze, E. Linder, and V. Umansky, *Phys. Rev. B* **62**, 10310 (2000).
- ¹³F. Stern, *Phys. Rev. Lett.* **21**, 1687 (1968).
- ¹⁴L. Smrcka and T. Jungwirth, *J. Phys.: Condens. Matter* **6**, 55 (1994).
- ¹⁵D. M. Whittaker, T. A. Fisher, P. E. Simmonds, M. S. Skolnick, and R. S. Smith, *Phys. Rev. Lett.* **67**, 887 (1991).
- ¹⁶L. V. Butov, A. V. Mintsev, Yu. E. Lozovik, K. L. Campman, and A. C. Gossard, *Phys. Rev. B* **62**, 1548 (2000); A. Parlange, P. C. M. Christianen, J. C. Maan, I. V. Tokatly, C. B. Soerensen, and P. E. Lindelof, *ibid.* **62**, 15323 (2000).
- ¹⁷M. Orlita, R. Grill, M. Zvara, G. H. Dohler, S. Malzer, M. Byszewski, and J. Soubusta, *Phys. Rev. B* **70**, 075309 (2004).
- ¹⁸A. I. Filin, I. V. Kukushkin, A. V. Larionov, and K. von Klitzing, *JETP Lett.* **61**, 706 (1995).
- ¹⁹M. Lax, *Phys. Rev.* **119**, 1502 (1960); V. N. Abakumov, V. I. Perel, and I. N. Yassievich, in *Nonradiative Recombination in Semiconductors*, edited by V. M. Agranovich and A. A. Maradudin, Modern Problems in Condensed Matter Sciences Vol. 33 (Elsevier, Amsterdam, 1991).
- ²⁰K. Seeger, *Semiconductor Physics* (Springer-Verlag, Berlin, 1982).
- ²¹C. Piermarocchi, F. Tassone, V. Savona, A. Quattropani, and P. Schwendimann, *Phys. Rev. B* **55**, 1333 (1997).
- ²²I. G. Lang, S. T. Pavlov, and A. V. Prokhorov, *Solid State Commun.* **8**, 639 (1993).
- ²³Y. V. Zhilyaev, V. V. Rossin, T. V. Rossina, and V. V. Travnikov, *JETP Lett.* **49**, 564 (1989).
- ²⁴P. S. Kop'ev, D. N. Mirlin, V. F. Sapega, and A. A. Sirenko, *JETP Lett.* **51**, 708 (1990).
- ²⁵B. I. Shklovskii, H. Fritzsche, and S. D. Baranovskii, *Phys. Rev. Lett.* **62**, 2989 (1989).
- ²⁶V. V. Rudenkov, P. C. M. Christianen, B. M. Ashkinadze, E. Cohen, J. C. Maan, and L. N. Pfeiffer (unpublished).
- ²⁷At 30 T, the lowest electron energy (0 Landau level) shifts by ~ 25 meV, and m_e increases by $<5\%$ due to conduction-band nonparabolicity. Such a nonparabolicity can be taken into account by a slight slope change (by 0.02 meV/T) for the studied B range.
- ²⁸M. S. Skolnick, A. K. Jain, R. A. Stradling, J. Leotin, J. C. Ouset, and S. Askenazy, *J. Phys. C* **9**, 2809 (1976).
- ²⁹W. Pan, K. Lai, S. P. Bayrakci, N. P. Ong, D. C. Tsui, L. N. Pfeiffer, and K. West, *Appl. Phys. Lett.* **83**, 3519 (2003).
- ³⁰S. I. Gubarev, T. Ruf, M. Cardona, and K. Ploog, *Phys. Rev. B* **48**, 1647 (1993).
- ³¹A. Baldareschi and N. C. Lipari, *Phys. Rev. B* **3**, 439 (1971).
- ³²I. Balslev, *Semicond. Sci. Technol.* **2**, 437 (1987).